Available online at www.sciencedirect.com

SCIENCE DIRECT®

Journal of Volcanology and Geothermal Research 137 (2004) 247–260

Journal of volcanology and geothermal research

www.elsevier.com/locate/jvolgeores

Thermodynamic modeling of post-entrapment crystallization in igneous phases

Victor C. Kress[a,*], Mark S. Ghiorso[b]

[a] *Earth and Space Sciences, University of Washington, Seattle, WA 98195, USA*
[b] *Geophysical Sciences, 5734 S. Ellis Ave., University of Chicago, Chicago, IL 60637, USA*

Abstract

Inclusions of quenched silicate liquid in igneous phenocryst phases represent important windows into the pre-eruption chemistry of volcanic rocks. Melt inclusions are subject to a variety of potential modifications after entrapment, which obscure the connection between final inclusion composition, and entrapment conditions. We concentrate on the effects of post-entrapment crystallization (PEC) in the cooling inclusion. PEC is neither an isobaric nor an isochoric process. Pressure decreases between 2 and 27 bars per degree of cooling, depending on the chemistry of melt and host and on the degree of PEC. In the equilibrium case, between about 50% and 65% of this pressure effect is due to thermal expansivity of the liquid, 10–35% from thermal expansivity of the host, and 5–40% from mass transfer between the inclusion and host. This complicates the application of simple element-partitioning schemes for back-calculating the effects of post-entrapment crystallization except in the simplest cases. We present a thermodynamic algorithm for PEC correction. This method is based on the self-consistent thermodynamic model set used in the MELTS software package. The algorithm moves backward through the PEC process, incrementally adding equilibrium crystal composition to the liquid while accounting for consequent variations in pressure and oxygen fugacity. Entrapment conditions are assumed to have been reached when the instantaneous liquidus solid composition most closely matches that of the bulk host crystal. Besides giving information on the degree of PEC and initial inclusion composition, the proposed algorithm can provide constraints on the pressure, temperature and oxygen fugacity at the time of entrapment. Olivine- and orthopyroxene-hosted inclusions from Popocatépetl, Mexico help constrain pre-eruption conditions for mixed magmas from recent eruptive products. Feldspar-hosted inclusions from Satsuma-Iwojima, Japan suggest that these magmas were substantially undersaturated with respect to supercritical vapor phase at the time of entrapment and underwent on the order of 29% post-entrapment crystallization. Quartz-hosted inclusions can potentially be employed in more silicic compositions, but this will require refinement of existing thermodynamic models.

Keywords: melt inclusions; post-entrapment crystallization; olivine; orthopyroxene; plagioclase; feldspar; Popocatépetl; Satsuma-Iwojima

1. Introduction

Igneous melt inclusions are found in a wide variety of magma types and host phenocryst phases (Roedder, 1979). The value of silicate melt inclusions as windows on pre-eruption conditions in igneous systems has been recognized for over 140 years (see references in Roedder, 1979). The proliferation and refinement of microbeam analytical techniques over the past three decades has revolutionized our ability to use melt-inclusion chemistry to determine pre-eruptive condi-

* Corresponding author. Fax: +1-206-543-0489.
E-mail address: kress@u.washington.edu (V.C. Kress).

0377-0273/$ - see front matter © 2004 Elsevier B.V. All rights reserved.
doi:10.1016/j.jvolgeores.2004.05.012

tions in igneous environments. In the ideal case, perhaps never fully realized in nature, the melt inclusion represents a quenched sample of the igneous melt phase present at the time of phenocryst growth. Since volcanic matrix glasses have nearly always undergone some degree of volatile loss during and after eruption, melt inclusions represent one of few practical means of sampling pre-eruption volatile chemistry in magmatic systems.

In this study, we use the term ''melt inclusion'' to refer to both the actual melts at the time of entrapment and their final glass form at the time of sampling and analysis. We consider only silicate melt inclusions.

A natural melt inclusion is likely to have been subjected to a variety of modifications during entrapment and while cooling. The usefulness of a melt inclusion with respect to deriving pre-eruption conditions is a function of the degree to which these modifications are either small enough to be ignored, or simple enough to be corrected.

Melt inclusions are usually formed by a crystal growth around a packet of melt. What starts as an embayment in the crystallization front can be completely closed off by subsequent crystal growth forming an isolated melt inclusion. These inclusions are generally small, meaning that the inclusion represents a sample of melt close to the crystal–liquid interface. If the crystal is growing rapidly, melt components not incorporated in the crystal structure will build up ahead of the growth front. This process is referred to as constitutional supercooling (Shewmon, 1983, p. 178). Constitutional supercooling is enhanced by rapid cooling, large contrast between melt and crystal composition, and slow diffusion. These same conditions may also enhance inclusion entrapment. Constitutional supercooling can potentially modify inclusion composition in a way that cannot generally be corrected. Fortunately, in cases where the possibility of compositional modification by constitutional supercooling has been considered, it has usually been found to be insignificant (Luhr, 2001; Lu et al., 1995; Roedder, 1979). These effects, along with other inclusion modifications related to magma mixing (Nakamura and Shimakita, 1998), will not be considered here.

As the trapped inclusion cools, the melt in the inclusion is no longer in equilibrium with its bulk host. This disequilibrium can drive diffusion of components into and out of the melt, modifying its original composition (Nielsen et al., 1998; Roedder, 1979; Qin et al., 1992; Danyushevsky et al., 2000). Formation of diffusive gradients within the host phenocryst due to partial re-equilibration during cooling may complicate the determination of pre-entrapment composition. In many such cases, careful characterization of gradients in the host and inclusion can be used to recover the original inclusion composition (Danyushevsky et al., 2000, 2002a). At slower cooling rates, diffusive gradients in the host phenocryst may extend to the host magma allowing incomplete or complete re-equilibration of the melt inclusion with host magma during cooling. This sort of open-system modification irretrievably erases information on inclusion composition at the time of entrapment. Gaetani and Watson (2000) show how olivine-hosted inclusions can show significant diffusive interaction with more evolved host magma at cooling rates as rapid as 1–2 °C/year.

Stresses induced during cooling can lead to fracturing, particularly in hosts that possess good or perfect cleavage (Roedder, 1979; Nielsen et al., 1998). Such fractures present a rapid conduit for post-entrapment volatile loss or other forms of chemical modification. For this reason, it is important to establish to the maximum degree possible that the particular inclusions being considered are intact in three dimensions (Roedder, 1979; Nielsen et al., 1998; Roedder, 1984).

It is well recognized that significant crystallization can occur on the walls of the inclusion after entrapment but prior to quenching. Several techniques have been developed to correct for this post-entrapment crystallization (PEC). The most direct means for PEC correction involves re-heating the inclusion on a microscope heating stage until the inclusion is homogenized (Danyushevsky et al., 1997; Sours-Page et al., 1999; Sinton et al., 1993). The greatest difficulty with this approach is determining the temperature of inclusion entrapment. Accurate knowledge of this temperature is necessary to determine at what temperature the annealing should be performed. Too low a temperature may leave PEC material unmelted, resulting in incomplete correction of the inclusion composition. An annealing temperature that is too high will add too much host composition to the inclusion, resulting in an inaccurate representation of pre-entrapment composition. Optimum temperature

can be obtained if the liquid was vapor saturated at the time of entrapment. In such a case, all that is required is to heat until vapor bubbles in the inclusion are eliminated (Danyushevsky et al., 2002a). Unfortunately, as will be shown later in this manuscript, it is not always obvious whether the assumption of vapor-saturation is valid. Vapor saturation can generally be assumed in cases where both fluid and melt inclusions coexist in a given growth zone in the same phenocryst. Nevertheless, any volatile loss during cooling, storage or annealing will result in annealing temperatures that are too low, and thus PEC corrections that are too small. Furthermore, extended annealing risks diffusive reaction between the inclusion and host resulting in composition profiles that are difficult or impossible to correct for. Such extended annealing is often employed to re-homogenize chemically inhomogeneous re-melted multi-phase inclusions.

We present an alternative technique for PEC correction which provides close constraints on entrapment temperature and composition. In many cases, this algorithm also provides information on pressure and oxygen fugacity at the time of entrapment as well. We consider only inclusions that have cooled rapidly enough that diffusive re-equilibration can be considered negligible. Practically, this criterion is most likely to be satisfied in rapidly quenched scoria, ash and pumice, though even rapidly quenched inclusions may have been influenced by diffusive re-equilibration during extended residence in magma chambers at depth.

2. Theory

We first define our system as a crystal-free melt inclusion of volume V with the system boundary formed by the inner wall of the host crystal. Our goal is to define an expression for pressure $P=P(T, V, \xi)$ where T is temperature, V is inclusion volume and ξ is a vector of component moles converted from liquid to solid. One approach to solving this problem exploits the fact that the inclusion is forced to be saturated in the host phase along its cooling path as long as the kinetics of crystallization are rapid enough to keep pace. Because the host phase is saturated along the PEC path, we can assume that the PEC path in P, T space must lie along the Clapeyron slope for the host phase. The difficulty arises in calculating the Clapeyron slope in complicated multicomponent liquids and solids. An elegant solution to this problem is presented by Walker et al. (1988). Unfortunately, implementation of this solution in the general case is difficult. We consider an alternative solution that lends further insight into details of the inclusion crystallization process. Both solutions support the conclusion that PEC is neither an isobaric nor isochoric process.

We can express small changes in $P(T, V, \xi)$ by the expression:

$$\mathrm{d}P = \left(\frac{\partial P}{\partial T}\right)_{V,\xi} \mathrm{d}T + \left(\frac{\partial P}{\partial V}\right)_{T,\xi} \mathrm{d}V + \left(\frac{\partial P}{\partial \xi}\right)_{T,V} \mathrm{d}\xi \tag{1}$$

V and ξ can be expressed as functions of T along the equilibrium crystallization path. This leads to:

$$\left(\frac{\partial P}{\partial T}\right)_{\Delta G} = \left(\frac{\partial P}{\partial T}\right)_{V,\xi} + \left(\frac{\partial P}{\partial V}\right)_{T,\xi} \left(\frac{\partial V}{\partial T}\right)_{\Delta G} + \left(\frac{\partial P}{\partial \xi}\right)_{T,V} \left(\frac{\partial \xi}{\partial T}\right)_{\Delta G}, \tag{2}$$

where the ΔG subscript indicates that the derivative is taken along the path of equilibrium crystallization (constant $\Delta G_{\mathrm{reaction}} = 0$). Given that host elasticity is more than an order of magnitude lower than that of the liquid, we make the simplifying assumption that elastic deformation of the host in response to pressure gradients is negligible to a first approximation. We further assume that thermal diffusion is rapid enough in inclusion and host that the effect of thermal gradients can be neglected.

Applying a bit of algebra and a few identities from calculus allows Eq. (2) to be expressed in terms of more commonly encountered thermodynamic variables:

$$\left(\frac{\partial P}{\partial T}\right)_{\Delta G} \simeq \frac{\alpha^{\mathrm{incl}}}{\beta_T^{\mathrm{incl}}} - \frac{\alpha^{\mathrm{host}}}{\beta_T^{\mathrm{incl}}} + \frac{\delta \bar{v}}{\beta_T^{\mathrm{incl}} V_T^{\mathrm{incl}}} \left(\frac{\partial \xi}{\partial T}\right)_{\Delta G}, \tag{3}$$

where $\alpha \equiv \frac{1}{V}\left(\frac{\partial V}{\partial T}\right)_P$, $\beta_T \equiv -\frac{1}{V}\left(\frac{\partial V}{\partial P}\right)_T$ and $\delta \bar{v}$ is a row vector with elements $\delta \bar{v}_i = \bar{v}_i^{\mathrm{incl}} - \bar{v}_i^{\mathrm{host}}$ for each component. x_i and $\bar{v}_i$ are mole fraction and partial molar volume for component i, and the superscripts incl and host refer to inclusion and host properties, respectively.

The first term on the right hand side of Eq. (3) expresses the pressure change induced by thermal contraction of the melt as it cools subject to a constant volume condition. The second addresses the pressure effect associated with changes in inclusion volume due to thermal contraction of the host. The final term in Eq. (3) expresses the pressure change induced by converting a given quantity of liquid to solid.

3. Application

Though Eq. (3) is useful to gain a perspective on the relative magnitude of contributions to pressure change during crystallization, it is not the most practical way of calculating PEC. The $(\partial\xi)/(\partial T)_{\Delta G}$ term in particular is difficult, though not impossible, to express in the general case. A far more practical solution is to solve the PEC problem numerically. To do this, we take advantage of the self-consistent set of thermodynamic models assembled in the MELTS package (Ghiorso and Sack, 1995). Our strategy is to work backward along the path of equilibrium crystallization from the observed composition of final quench to an estimate of the temperature, pressure, oxygen fugacity and composition of initial entrapment. A flow chart for the algorithm employed is shown in Fig. 1.

Initial input to the program includes the measured inclusion composition and the composition of the host crystal at a point judged to represent the composition of the crystal at the time of entrapment. The host composition can be a composition measured far enough from the inclusion to be free of the influence of PEC or phase edges, but at the same position in the crystal zoning profile (if any) as the inclusion. The algorithm outlined in Fig. 1 also requires an initial guesses for pressure and relative oxygen fugacity[1] at the time PEC was completed (i.e. quench).

Using input temperature, pressure and composition data, the implementation program first constructs

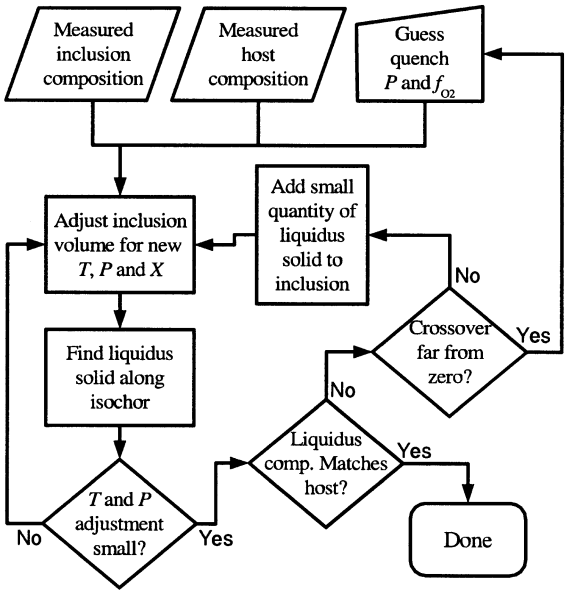

Fig. 1. Flow chart for numerical calculation of initial composition of the inclusion at the time of entrapment. See text for explanation.

thermodynamic representations of host and inclusion respectively in the form of model objects on the computer. These model objects provide self-consistent and thermodynamically valid mathematical representations of the response of the thermodynamic state of the phase in question to variations in composition, pressure, temperature, volume, etc. This allows relatively straightforward calculation of thermodynamic quantities required in the numerical calculations outlined in Fig. 1.

Once initialization is complete, the inclusion model is used to calculate isochorically the saturation temperature and liquidus crystal composition for the host phase. This liquidus crystal composition represents the composition of the host phase in equilibrium with the inclusion at the saturation temperature. We will refer to this liquidus phase the "instantaneous host". At this initial stage, the calculated instantaneous host composition will only match the measured host composition if all relevant assumptions hold, no PEC has taken place in the inclusion and our quench pressure and fugacity guesses are correct.

The next step in the calculation is to add a small quantity of this instantaneous host to the inclusion and adjust inclusion volume, temperature, pressure and composition for consistency. This process is repeated

[1] It has been verified experimentally that lines of constant ferric/ferrous iron ratio in silicate melts in $f_{O_2}-T-P$ space roughly parallel solid oxygen buffers such as Ni–NiO and fayalite–magnetite–quartz (Sato, 1978; Sack et al., 1980; Kress and Carmichael, 1988, 1991). Thus, oxygen fugacity relative to these solid buffers is a useful coordinate of melt redox state that is approximately independent of temperature or pressure.

in small increments of increasing temperature, leading to continuous variations in inclusion composition, volume, pressure and oxygen fugacity. When the composition of the instantaneous host closely matches the measured host composition, we can take the temperature, pressure composition and f_{O_2} of the inclusion object at that iteration as good estimates of corresponding conditions at the time of entrapment. If the composition never matches along the chosen path, they can often be brought into better agreement by adjusting initial guesses for pressure and oxygen fugacity and re-starting the process. The fraction crystallized is merely the sum of the weight of instantaneous host added over all iterations divided by the initial weight of the inclusion.

In principle, this approach can be applied to silicate inclusions in any phase for which a self-consistent thermodynamic model is available. All that is required is that the inclusion remained closed with respect to everything but crystallization, that that crystallization is monomineralic.

We implicitly assume in this approach that PEC is a fractional process. In other words, we assume that, after precipitation, each layer of incremental solid does not diffusively interact with the melt inclusion, bulk host or matrix magma. The validity of these assumptions must be tested for each application.

3.1. Olivine-hosted inclusions

Olivine is a useful host for melt inclusions due to its early and prominent occurrence in a variety of mafic extrusives. The usefulness of olivine as a inclusion host is enhanced by its imperfect cleavage, making inclusions less subject to fracture and leakage. Furthermore, the relatively simple chemistry of olivine facilitates PEC correction of inclusion chemistry. The cation exchange reaction:

$$Mg_2SiO_4^{olivine} + FeO^{liquid} \rightleftharpoons Fe_2SiO_4^{olivine} + MgO^{liquid} \quad (4)$$

is relatively independent of temperature (Roeder and Emslie, 1970; Ulmer, 1989; Ford et al., 1983; Longhi et al., 1978) and is not strongly dependent on pressure (Ulmer, 1989; Ford et al., 1983). If one assumes that PEC is fast enough to be considered fractional, then both melt inclusion composition and the instantaneous precipitated host composition will evolve to higher Fe/(Fe+Mg) as PEC proceeds (Fig. 2). The Fe–Mg exchange method for PEC correction (Gaetani and Watson, 2000; Luhr, 2001; Metrich and Clocchiatti, 1996; Harris and Anderson, 1983; Cervantes and Wallace, 2003; Sisson and Layne, 1993) works backward through the PEC process illustrated in (Fig. 2) by incrementally adding a small amount of the presumed equilibrium instantaneous olivine to the melt until the instantaneous olivine matches the host. In this way, final measured inclusion composition (point A in Fig. 2) and host crystal (point B in Fig. 2) are used to estimate the unknown degree of PEC (unscaled x axis in Fig. 2), and the unknown initial composition of the inclusion at the time of entrapment (point C in Fig. 2). This technique provides estimates of the degree of PEC and the initial composition of the inclusion. It gives no information regarding conditions of entrapment. The cation exchange approach is successful only to the extent that reaction (4) can be considered independent of pressure, temperature oxygen fugacity and composition.

The PEC correction scheme advocated here is, at its core, similar to the Fe–Mg exchange approach described in the previous paragraph except that we consider evolution of component abundances rather than Fe/Mg ratios, and exchange equilibrium is esti-

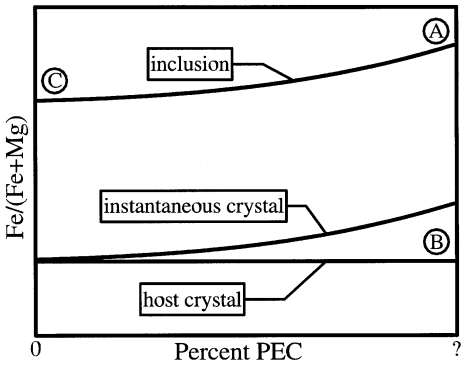

Fig. 2. Evolution of Fe/(Fe+Mg) at three points as a function of PEC (increasing to right) in an idealized olivine-hosted inclusion. "Host crystal" is composition of host crystal away from inclusion but on same growth zone. "Instantaneous host" is the composition of last precipitated solid, which is assumed to be host phase in equilibrium with inclusion composition at the time of precipitation. "Inclusion" is the composition of the melt inclusion, which is assumed to be homogeneous.

mated using self-consistent thermodynamic models. Because most natural olivines lie very close to the forsterite-fayalite binary and reaction (4) is not a strong function of pressure or temperature, the Fe–Mg exchange approach and the approach described here can be expected to give similar results. Because temperature is explicitly tracked along the PEC path, the algorithm presented here provides an estimate of the temperature of entrapment. Furthermore, because the model we employ to establish equilibrium (MELTS) explicitly accounts for subtle but real variations in reaction (4) as a function of P, T, composition and f_{O_2}, one can hope to extract more accurate initial inclusion compositions as well as information regarding pressure and redox conditions of entrapment.

To illustrate how one would apply PEC corrections to olivine-hosted inclusions, we consider a mafic olivine-hosted inclusion from 30 June 1997 Popocatépetl mixed brown andesite pumice (Witter et al., 2004b; Witter, 2003, inclusion MI2ol17tsSCa). All inclusions in this study were carefully examined for intersecting cracks or necks that might have facilitated loss of more mobile components. Detailed microprobe scans verified that there was no detectable compositional gradient in the host radial to the inclusion. Though small portion of this inclusion was removed during thin-section preparation and could not be examined, there was no evidence of bubbles or other solid phases in the inclusion. Inclusion composition (Table 1) was determined by electron microprobe except water, which was determined by difference. Analytical methods are described in detail in Witter et al. (2004b) and Witter (2003).

Table 1
Measured and PEC-corrected compositions for olivine-hosted inclusion MI2ol17tsSCa from Witter et al. (2004b) and Witter (2003) in normalized wt.%

	Measured	PEC-corrected
SiO_2	57.2	56.0
TiO_2	1.17	1.10
Al_2O_3	18.1	16.90
FeO*	5.44	6.37
MnO	0.12	0.13
MgO	2.58	5.06
CaO	7.60	7.12
Na_2O	4.40	4.11
K_2O	1.48	1.38
P_2O_5	0.27	0.25
H_2O	1.4	1.3
S (ppm)	1130	1057
Cl (ppm)	712	666
F (ppm)	686	642

Fig. 3 is a plot of the difference between the calculated instantaneous equilibrium olivine composition and the measured host composition as a function of temperature for the inclusion in Table 1 calculated using the algorithm presented above. In this representation, equilibrium between instantaneous precipitating olivine and the bulk host would be expressed by zero $X_{\text{inst.}} - X_{\text{host}}$ values for all components. Thus, if the PEC correction algorithm is correctly applied, all curves on in Fig. 3 should converge to zero at the same temperature. This zero intersection temperature would correspond to the temperature at which the melt inclusion was initially isolated from the bulk liquid (the entrapment temperature). The degree to which this crossover deviates from zero is a measure of the degree to which our initial guesses, thermodynamic models or assumptions are not correct. Minor components, such as Ni-olivine in Fig. 3, are often dominated by analytical and model error and give little useful information on PEC conditions. In the case of forsterite and fayalite components in Fig. 3, the crossover point can be moved upward and to the right by either increasing the initial pressure estimate or increasing the estimated relative oxygen fugacity. Whether such adjustments are reasonable must be evaluated in the context of outside constraints obtained from fluid inclusions or the sample assemblage as a whole. In the absence of such external constraints, entrapment pressure and oxygen fugacity cannot be independently resolved. If such adjustments are not reasonable, then one must conclude that the closed-system fractional crystallization assumption is not warranted. No such self-consistency check exists for the simpler Fe–Mg exchange technique for estimation of PEC. For the case illustrated in Fig. 3, a reasonable crossover value can be obtained assuming a quench pressure of 5 kbars and a relative oxygen fugacity of about 0.6 log unit below Ni–NiO. We estimate that this inclusion was trapped at about 1173 °C and that PEC continued during cooling to about 1040 °C.

Fig. 4 shows calculated pressure and percent crystallized as a function of temperature for the case considered in Fig. 3. Results suggest that the inclusion had crystallized about 7.3% and that inclusion pres-

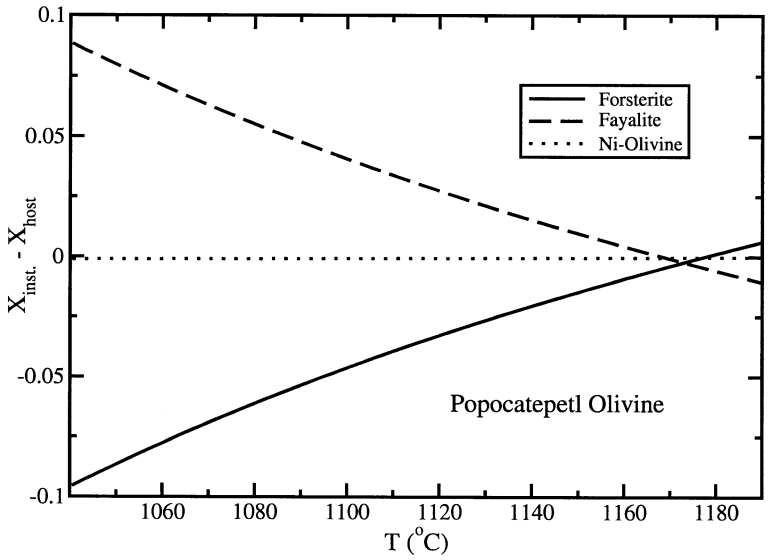

Fig. 3. Difference between instantaneous equilibrium olivine composition and host olivine composition in mole fractions as a function of temperature for olivine-hosted inclusion in 30 June 1997 Popocatépetl mixed brown andesite pumice (Witter et al., 2004b).

sure decreased about 276 bars between entrapment and final quench. The estimated entrapment pressure of 5.3 kbars is consistent with other petrographic constraints from these rocks (Witter et al., 2004b; Witter, 2003). For this Popocatépetl example, $\partial P/\partial T$ at the point of entrapment is on the order of 3.1 bars/K. The first term of Eq. (3) contributes about 58% of the pressure effect, the second term contributes about 31% and the final term 11%. $\partial P/\partial T$ estimates for inclusions from other Popocatépetl olivines range between 2 and over 4 bars/K depending on melt composition and degree of PEC.

The algorithm presented in this study explicitly tracks relative oxygen fugacity as a function of PEC. In the case described above, the calculated relative oxygen fugacity only increases 0.33 $\log_{10}$ units over

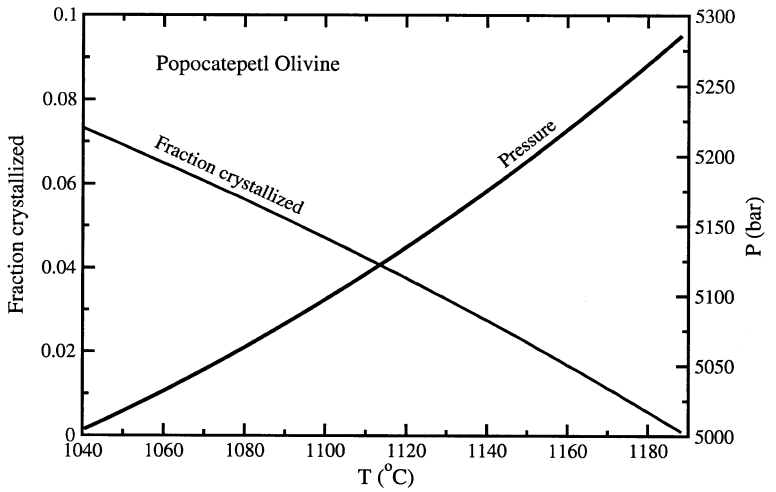

Fig. 4. Pressure and percent crystallized as function of temperature for olivine-hosted inclusion considered in Fig. 3 (Witter et al., 2004b).

the estimated 7.3% crystallization. Entrapment at 0.9 log units below Ni–NiO is consistent with other constraints from these rocks (Witter et al., 2004b). Quite large degrees of PEC are required to influence the relative oxygen fugacity of the inclusion by a measurable amount. This suggests that redox indicators such as Fe (Fudali, 1965; Gaillard et al., 2001; Kilinc et al., 1983; Kress and Carmichael, 1991; Ottonello et al., 2001; Sack et al., 1980) or S (Carroll and Rutherford, 1988; Wallace and Carmichael, 1994) could be used to deduce the oxygen fugacity at the time of entrapment if relevant micro-analytical obstacles can be overcome.

Comparison of PEC fraction estimates using the algorithm presented here with the Fe–Mg distribution approach for a large number of relatively reduced olivine-hosted inclusions trapped at moderate pressures using K_D values from Roeder and Emslie (1970) suggests that the two methods predict crystallization fractions that differ by less than 0.5% (J.B. Witter, 2002, pers. comm.). The primary advantages of the more complicated approach described here are that (1) it provides additional information about intensive variables at the time of entrapment; (2) it can be applied over a broader composition range; and (3) it can be applied in phases with more complicated chemistry than olivine.

3.2. Orthopyroxene-hosted inclusions

The kinetics of orthopyroxene equilibration is significantly slower than olivine, decreasing the potential for diffusive open-system behavior during cooling. On the other hand, orthopyroxene has better cleavage than olivine, increasing the potential for post-entrapment volatile leakage.

The chemistry of orthopyroxene is considerably more complicated than that of olivine. Because of this, the simple cation exchange method used to calculate PEC in olivines cannot be easily applied in orthopyroxene-hosted inclusions. On the other hand, because the chemistry of melt-pyroxene equilibrium is more dependent on pressure, temperature and composition than the olivine case, our technique provides less ambiguous constraints on entrapment pressure and oxygen fugacity conditions in pyroxene-hosted inclusions. Self-consistent thermodynamic models for orthopyroxene and liquid are available (Sack, 1980; Sack and Ghiorso, 1994, 1989; Ghiorso and Sack, 1995). Thus, application of the PEC algorithm presented in this study to orthopyroxene-hosted inclusions is no more difficult than application to olivine-hosted inclusions.

We consider an orthopyroxene-hosted inclusion (MI1opx8tsSCa) from a more silicic region of the same 30 June 1997 Popocatépetl mixed brown andesite pumice that hosted the olivine-hosted example considered above (Witter et al., 2004b; Witter, 2003). As in the olivine case, orthopyroxene-hosted inclusions from this study were carefully examined for intersecting fractures, radial composition gradients and multiple phase saturation. Pre- and post-correction compositions for this inclusion are in Table 2.

Fig. 5 shows the difference between instantaneous liquidus orthopyroxene and bulk host crystal for inclusion MI1opx8tsSCa. Pyroxene compositions are expressed here in terms of a minimal independent set of components (Sack and Ghiorso, 1994). Expressed in this way, component concentration coordinates may have positive or negative values. Only the five most significant components are considered. As in the olivine case, the primary adjustment in composition during PEC correction involves Fe–Mg exchange, expressed here in variations in diopside and hedenbergite components. Other components remain relatively constant and offset from zero. This offset may be a consequence of analytical error, incorrect initial conditions, failure

Table 2
Measured and PEC-corrected compositions for orthopyroxene-hosted inclusion MI1opx8tsSCa from Witter et al. (2004b) and Witter (2003) in normalized wt.%

	Measured	PEC-corrected
SiO_2	71.1	70.7
TiO_2	0.41	0.40
Al_2O_3	12.3	12.0
FeO*	3.56	4.02
MnO	0.07	0.07
MgO	0.85	1.42
CaO	2.24	2.20
Na_2O	3.71	3.62
K_2O	2.46	2.40
P_2O_5	0.32	0.30
H_2O	2.8	2.7
S (ppm)	163	159
Cl (ppm)	929	905
F (ppm)	692	675

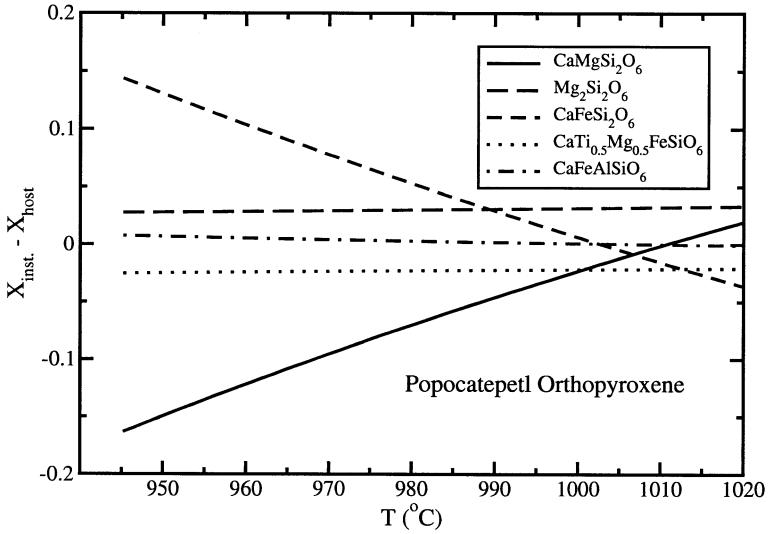

Fig. 5. Difference between instantaneous equilibrium orthopyroxene composition and host orthopyroxene composition in mole fractions as a function of temperature for orthopyroxene-hosted inclusion from more felsic region of same 30 June 1997 Popocatépetl mixed brown andesite pumice considered in Fig. 3 (Witter et al., 2004b).

of model assumptions or flaws in the thermodynamic models. In any case, the magnitude of the offset is small relative to the major features of this plot.

The inclusion shown in Fig. 5 is best modeled assuming entrapment occurred at 1008 °C at pressures less than 0.1 GPa. As in the case of the olivine plot, increasing oxygen fugacity drives the crossover point toward more positive values. The optimum oxygen fugacity is close to the Ni–NiO buffer. These results are toward the high end of temperatures and low end of oxygen fugacities derived from two-pyroxene thermometry and Fe–Ti oxides in these rocks (Witter et al., 2004b) but they are consistent within error. Modeling suggests that roughly 3% PEC took place over 65 °C of cooling. Pressure decreased roughly 17 bars/K over this range. About 67% of this pressure effect can be attributed to inclusion thermal expansivity, 25% to host thermal expansion and 8% to mass transfer. The relative oxygen fugacity increased by only about 0.1 $\log_{10}$ units as a consequence of PEC.

Inclusions from the olivine considered above and the orthopyroxene considered here suggest significantly different entrapment conditions for two inclusions from the same hand specimen. This conclusion is consistent with other observations from this sample. Host phenocrysts in this sample are clearly out of equilibrium with each other, with clear textural evidence for magma mingling. Inclusion data such as those considered here were used, along with other data from these rocks, to deduce pre-mixing compositions and conditions for the basaltic and dacitic end-members in this mixing event (Witter et al., 2004b; Witter, 2003). Accurate recovery of pre-mixing volatile compositions allowed constraints to be made on volatile budget and degassing conditions for the most recent volcanic activity at Popocatépetl (Witter et al., 2004b; Witter, 2003).

3.3. Feldspar-hosted inclusions

Feldspar is an abundant phenocryst phase in most extrusive igneous rocks. Feldspar-hosted melt inclusions are common. The usefulness of feldspar-hosted phenocrysts is reduced somewhat by feldspar's perfect cleavage which increases the potential for decrepitation of volatile species. The potential for volatile loss is further enhanced by the rapid rate of diffusion in feldspars relative to other potential host phenocrysts.

Saito et al. (2001) undertook a detailed study of melt inclusions from Satsuma-Iwojima, Japan in order to explore volatile evolution in the underlying magma chamber. They considered 30 inclusions

hosted by plagioclase, orthopyroxene and clinopyroxene. Inclusion compositions are well characterized for major element oxides, H_2O, CO_2, S and Cl. Plagioclase-hosted inclusions from this study are of particular interest here, as inclusion compositions suggest anorthoclase or oligoclase on the liquidus, while hosts have anorthite contents between 47% and 65%. Saito et al. (2001) do not discuss this apparent contradiction.

We consider an An57 plagioclase-hosted inclusion from the 6300 years BP Takashima pyroclastic flow deposit (Saito et al., 2001, inclusion 2406A). This inclusion is 210 × 100 μm homogeneous glass, without vapor bubbles. On the basis of their measured 3.8 wt.% water content in this inclusion, Saito et al. (2001) concluded that entrapment pressure was likely to have been greater than about 1.3 kbars at the time of quench. We use their minimum pressure estimate as an initial pressure in our calculations. We arbitrarily assume that this inclusion quenched at Ni–NiO, but calculations in feldspar-hosted low-iron silicic inclusions are insensitive to redox state.

Results of PEC correction suggest that the inclusion was trapped at about 3 kbars and 1029 °C (Fig. 6). At the time of entrapment, this inclusion contained about 2.9% H_2O and 66.7% SiO_2. PEC proceeded over 189 °C of cooling decreasing pressure by 57% and leading to a total of about 29% crystallization. Similar results were obtained for other inclusions from this unit. $\partial P/\partial T$ in this example is estimated to be on the order of 12 bars/K at the time of entrapment, dropping to about 9 bars/K at quench. This value for $\partial P/\partial T$ at entrapment is more than three times the corresponding value estimated in the olivine example. Fifty-four percent of the pressure effect in this feldspar-hosted inclusion can be attributed to inclusion thermal expansion, 12% to host thermal expansion and 34% to mass transfer. It is interesting to note that similar calculations on basaltic-andesite inclusions in feldspars from Villarrica, Chile (Witter et al., 2004a; Witter, 2003) suggest PEC-induced pressure effects as high as 27 bars/K.

Application of PEC correction to this Takashima inclusion results in a 28% decrease in the estimated water content of this magma at the time of entrapment (Table 3). Saito et al. (2001) concluded in their study that these inclusions were water saturated at the time of entrapment, and that variations in water content among these samples reflect variations in entrapment pressures. In contrast, our results suggest that these magmas were significantly undersaturated at the time of

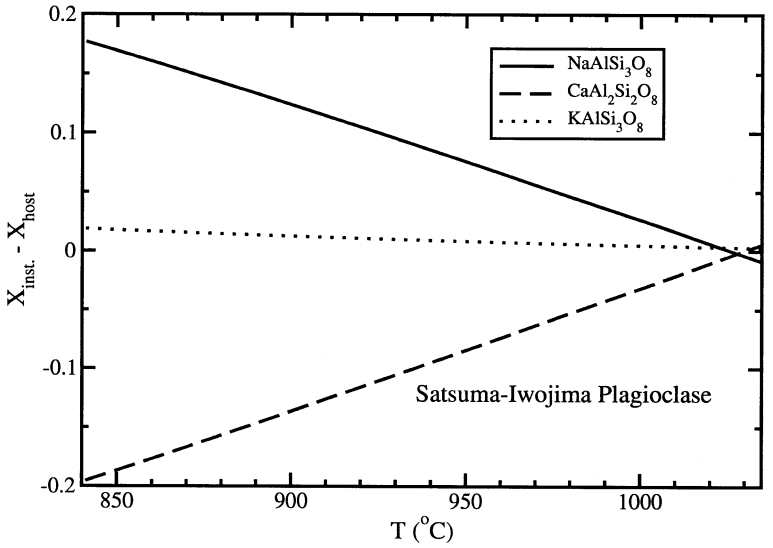

Fig. 6. Difference between instantaneous equilibrium plagioclase composition and host plagioclase composition as function of temperature from dacite inclusion (2406A) hosted by An57 plagioclase from the 6300 years BP Takashima pyroclastic flow deposit (Saito et al., 2001).

Table 3
Measured and PEC-corrected compositions for feldspar-hosted inclusion 2406A from Saito et al. (2001) in normalized wt.%

	Measured	PEC-corrected
SiO_2	70.80	66.73
TiO_2	0.74	0.53
Al_2O_3	12.66	16.90
FeO*	2.75	1.98
MnO	0.08	0.06
MgO	0.66	0.48
CaO	2.07	4.25
Na_2O	3.28	3.98
K_2O	2.79	2.10
H_2O	3.99	2.88
CO_2 (ppm)	<39	<30
S (ppm)	180	137
Cl (ppm)	1500	1141

entrapment, and that variations in water to a large extent reflect variations in thermal history and PEC. This is a good example of a case where more sophisticated treatment of PEC can both qualitatively and quantitatively change our understanding of pre-eruption conditions.

3.4. Quartz-hosted inclusions

Quartz phenocrysts in silicic igneous rocks provide a potentially valuable host for melt inclusions. The lack of cleavage in this mineral reduces the potential for inclusion fracturing and leakage. Strong evidence for PEC in quartz phenocrysts from the Bishop Tuff has been observed using cathodeluminescence imaging (Peppard et al., 2001). Unfortunately, because the quartz host is a single-component system, the composition of the instantaneous host will always match that of the host. We cannot, therefore, employ the methods described above to unambiguously estimate the degree of PEC, melt chemistry at the time of entrapment or conditions at the time of entrapment. This does not mean that the PEC algorithm cannot be profitably employed in quartz-hosted inclusions. Most quartz-saturated volcanic rocks are also saturated in other phases such as plagioclase or pyroxene. If we assume or can establish that these phases were saturated at the time of entrapment, we can plot the chemical affinity of the second phenocryst phase as a function of temperature along the PEC correction path. Chemical affinity is a scalar thermodynamic measure of the degree to which a given phase is undersaturated or supersaturated at a given set of conditions. In the ideal application, the second phenocryst phase will be just saturated (affinity will be zero) at the conditions of entrapment. Unfortunately, attempts to apply this technique to feldspar- and opx-bearing samples from the Bishop Tuff (Wallace et al., 1999; Hildreth, 1979; Wilson and Hildreth, 1997) and the Valley of Ten Thousand Smokes (Hildreth, 1983; Lowenstern, 1993) have not been successful. We attribute this lack of success to inadequate calibration of the thermodynamic models in these high-silica and low MgO/(FeO + MgO) compositions. Refinement of these models in the future should allow successful application of the technique presented here in quartz-hosted inclusions.

4. Summary and qualifications

The melt inclusions that we are considering represent equilibrium between only two phases in a many-component system. As such, the system has high variance in a phase-rule sense. Consequently, constraints on entrapment conditions may be very weak and highly dependent on estimates of other intensive variables. Judgment must be exercised to distinguish interpretations that are well constrained by the data from those that are generated from open-system processes, analytical uncertainty or correlation between poorly constrained variables. Achieving tight constraints on entrapment conditions will usually require the application of additional constraints on intensive variables from the petrologic context of the host crystal. This tool is a supplement to, not a replacement for, other petrological and analytical techniques.

This approach is developed under the assumption that, after entrapment, the inclusion remained a closed system with respect to everything but PEC. As with any technique involving melt inclusions, volatile leakage through fractures, diffusive hydrogen loss or diffusion of other melt components into or out of the host phase can reduce the validity of this approach.

Though the effects if major-element diffusion can be partially corrected with detailed work (Danyushevsky et al., 2000, 2002b,a), hosts from rapidly quenched scoria or ash will provide the most reli-

able inclusion compositions (Luhr, 2001). Rapidly quenched samples are not guaranteed to be free of post-entrapment modification by diffusion, as phenocrysts may reside for considerable time in the magma chamber prior to eruption. Clearly, where there are measurable composition gradients in the host radial to the inclusion, results should be considered highly suspect. The PEC algorithm presented here will probably not be sensitive to post-entrapment diffusion on the ≈ 10 μm scale, as reference melt and host compositions measured farther away from inclusion walls are no likely to be strongly effected. Fortunately, this is about the scale of resolvable profiles on the electron microprobe. The influence of such minor diffusive re-equilibration will likely be somewhat larger in laboratory re-homogenization techniques as prolonged heating may generate further diffusion and the effects of diffusion will increase empirically determined homogenization temperatures (Danyushevsky et al., 2000).

The technique presented here does not lend itself to application in multi-phase inclusions. In principle, it would be possible to apply this technique in multiphase inclusions if it were possible to establish accurately the composition and relative volumes of all phases in the inclusion. Unfortunately, such cases are rare in practice. Though it is not uncommon for workers to correct for second-phase saturation where bubbles are the second phase, such corrections can add substantial error and ambiguity to inclusion analysis. Where possible, it is best to consider only inclusions that have quenched fast enough to avoid saturation with other phases (including bubbles). Where multiple-phase inclusions are unavoidable, minimal annealing followed by analysis and application of this algorithm is probably the best approach.

Finally, in selecting inclusions, it is important to consider the potential for disequilibrium compositions in inclusions that formed by dissolution followed by recrystallization (Nakamura and Shimakita, 1998). With these qualifications in mind, detailed thermodynamic treatment of melt inclusions in igneous phenocryst phases can provide a wealth of information that cannot be obtained in any other way. Executable versions of the programs used in this study will be made available for the Linux and Macintosh OSX platforms through the MELTS web site.

Acknowledgements

This manuscript was greatly enhanced by careful, constructive and critical reviews by L. Danyuschevsky, M. Rutherford and R. Nielson. Thanks to Jeffrey Witter for suffering through buggy early versions of this program during his PhD research. Work was supported primarily through NSF-EAR-9980566 to Kress and C.G. Newhall and EAR 62-2536 to Ghiorso and Kress.

References

Carroll, M.R., Rutherford, J., 1988. Sulfur speciation in hydrous experimental glasses of varying oxidation state: results from measured wavelength shifts of sulfur X-rays. American Mineralogist 73, 845–849.

Cervantes, P., Wallace, P., 2003. Magma degassing and basaltic eruption styles: a case study of 2000 year BP Xitle volcano in central Mexico. Journal of Volcanology and Geothermal Research 120, 249–270.

Danyushevsky, L.V., Carroll, M.R., Fanning, J.C., 1997. Origin of high-An plagioclase in Tongan high-Ca boninites: implications for plagioclase-melt equilibria at low $P(H_2O)$. Canadian Mineralogist 35, 313–326.

Danyushevsky, L.V., Della-Pasqua, F.N., Sokolov, S., 2000. Re-equilibration of melt inclusions trapped by magnesian olivine phenocrysts from subduction-related magmas: petrological implications. Contributions to Mineralogy and Petrology 138, 68–83.

Danyushevsky, L.V., McNeill, A.W., Sobolev, A.V., 2002a. Experimental and petrological studies of melt inclusions in phenocrysts from mantle-derived magmas: an overview of techniques, advantages and complications. Chemical Geology 183, 5–24.

Danyushevsky, L.V., Sokolov, S., Falloon, T.J., 2002b. Melt inclusions in olivine phenocrysts: using diffusive re-equilibration to determine the cooling history of a crystal, with implications for the origin of olivine-phyric volcanic rocks. Journal of Petrology 43 (9), 1651–1671.

Ford, C.E., Russell, D.G., Craven, J.A., Fisk, M.R., 1983. Olivine–liquid equilibria: temperature, pressure and composition dependence of the crystal/liquid cation partition coefficients for Mg, Fe^{3+}, Ca and Mn. Journal of Petrology 3, 256–265.

Fudali, R.F., 1965. Oxygen fugacities of basaltic and andesitic magmas. Geochimica et Cosmochimica Acta 29, 1063–1075.

Gaetani, G.A., Watson, E.B., 2000. Open system behavior of olivine-hosted melt inclusions. Earth and Planetary Science Letters 183, 27–41.

Gaillard, F., Scaillet, B., Pichavant, M., Bény, J.-M., 2001. The effect of water and f_{O_2} on the ferric–ferrous ratio of silicic melts. Chemical Geology 174, 255–273.

Ghiorso, M.S., Sack, R.O., 1995. Chemical mass transfer in mag-

matic processes: IV. A revised and internally consistent thermodynamic model for the interpolation and extrapolation of liquid–solid equilibria in magmatic systems at elevated temperatures and pressures. Contributions to Mineralogy and Petrology 119, 197–212.

Harris, D.M., Anderson, A.T., 1983. Concentrations, sources, and losses of H_2O, CO_2 and S in Kilauean basalt. Geochimica et Cosmochimica Acta 47, 1139–1150.

Hildreth, W., 1979. The Bishop Tuff: evidence for the origin of compositional zonation in silicic magma chambers. Special Paper - Geological Society of America 180, 43–75.

Hildreth, W., 1983. The compositionally zoned eruption of 1912 in the Valley of Ten Thousand Smokes, Katmai National Park, Alaska. Journal of Volcanology and Geothermal Research 18, 1–56.

Kilinc, A., Carmichael, I.S.E., Rivers, M.L., Sack, R.O., 1983. The ferric–ferrous ratio of natural silicate liquids equilibrated in air. Contributions to Mineralogy and Petrology 83, 136–140.

Kress, V.C., Carmichael, I.S.E., 1988. Stoichiometry of the iron oxidation reaction in silicate melts. American Mineralogist 73, 1267–1274.

Kress, V.C., Carmichael, I.S.E., 1991. The compressibility of silicate liquids containing Fe_2O_3 and the effect of composition, temperature, oxygen fugacity and pressure on their redox states. Contributions to Mineralogy and Petrology 108, 82–92.

Longhi, J., Walker, D., Hays, J.F., 1978. The distribution of Fe and Mg between olivine and lunar basaltic liquids. Geochimica et Cosmochimica Acta 42, 1545–1558.

Lowenstern, J.B., 1993. Evidence for a copper-bearing fluid in magma erupted at the Valley of Ten Thousand Smokes, Alaska. Contributions to Mineralogy and Petrology 114, 409–421.

Lu, F., Anderson, A.T., Davis, A.M., 1995. Diffusional gradients at the crystal/melt interface and their effect on the composition of melt inclusions. Journal of Geology 103, 591–597.

Luhr, J.F., 2001. Glass inclusions and melt volatile contents at Parícutin Volcano, Mexico. Contributions to Mineralogy and Petrology 142, 261–283.

Metrich, N., Clocchiatti, R., 1996. Sulfur abundance and its speciation in oxidized alkaline melts. Geochimica et Cosmochimica Acta 60 (21), 4151–4160.

Nakamura, M., Shimakita, S., 1998. Dissolution origin and syn-entrapment compositional change of melt inclusion in plagioclase. Earth and Planetary Science Letters 161, 119–133.

Nielsen, R.L., Michael, P.J., Sours-Page, R., 1998. Chemical and physical indicators of compromised melt inclusions. Geochimica et Cosmochimica Acta 62 (5), 831–839.

Ottonello, G., Moretti, R., Marini, L., Zuccolini, M.V., 2001. Oxidation state of iron in silicate glasses and melts: a thermochemical model. Chemical Geology 174, 157–179.

Peppard, B.T., Steele, I.M., Davis, A.M., Wallace, P.J., Anderson, A.T., 2001. Zoned quartz phenocrysts from the rhyolitic Bishop Tuff. American Mineralogist 86, 1034–1052.

Qin, Z., Lu, F., Anderson, A.T.J., 1992. Diffusive reequilibration of melt and fluid inclusions. American Mineralogist 77, 565–576.

Roedder, E., 1979. Origin and significance of magmatic inclusions. Bulletin de Minéralogie 102, 487–510.

Roedder, E., 1984. Fluid Inclusions. Reviews in Mineralogy, vol. 12. Mineralogical Society of America, Washington, DC, 646 pp.

Roeder, P.L., Emslie, R.F., 1970. Olivine–liquid equilibrium. Contributions to Mineralogy and Petrology 29, 275–280.

Sack, R.O., 1980. Some constraints of the thermodynamic mixing properties of Fe–Mg orthopyroxenes and olivines. Contributions to Mineralogy and Petrology 71, 257–269.

Sack, R.O., Ghiorso, M.S., 1989. Importance of considerations of mixing properties in establishing an internally consistent thermodynamic database: thermochemistry of minerals in the system Mg_2SiO_4–Fe_2SiO_4–SiO_2. Contributions to Mineralogy and Petrology 102, 41–68.

Sack, R.O., Ghiorso, M.S., 1994. Thermodynamics of multicomponent pyroxenes: I. Formulation of a general model. Contributions to Mineralogy and Petrology 116, 277–286.

Sack, R.O., Carmichael, I.S.E., Rivers, M., Ghiorso, M.S., 1980. Ferric–ferrous equilibria in natural silicate liquids at 1 bar. Contributions to Mineralogy and Petrology 75, 369–376.

Saito, G., Kazahaya, K., Shinohara, H., Stimac, J., Kawanabe, Y., 2001. Variation of volatile concentration in a magma system of Satsuma-Iwojima volcano deduced from melt inclusion analysis. Journal of Volcanology and Geothermal Research 108, 11–31.

Sato, M., 1978. Oxygen fugacity of basaltic magmas and the role of gas-forming elements. Geophysical Research Letters 6, 447–449.

Shewmon, P.G., 1983. Transformations in Metals. J. Williams Book, Jenks, OK, 394 pp.

Sinton, C.W., Christie, D.M., Coombs, V.L., Nielsen, R.L., Fisk, M.R., 1993. Near-primary melt inclusions in anorthite phenocrysts from the Galapagos Platform. Earth and Planetary Science Letters 119, 527–537.

Sisson, T.W., Layne, G.D., 1993. H_2O in basalt and basaltic andesite glass inclusions from four subduction-related volcanoes. Earth and Planetary Science Letters 117, 619–635.

Sours-Page, R., Johnson, K.T.M., Nielsen, R.L., Karsten, J.L., 1999. Local and regional variation of MORB parent magmas: evidence from melt inclusions from the Endevour Segment of the Juan de Fuca Ridge. Contributions to Mineralogy and Petrology 134, 342–363.

Ulmer, P., 1989. The dependence of the Fe^{2+}–Mg cation-partitioning between olivine and basaltic liquid on pressure, temperature and composition. An experimental study to 30 kbars. Contributions to Mineralogy and Petrology 101, 261–273.

Walker, D., Agee, C.B., Zhang, Y., 1988. Fusion curve slope and crystal/liquid buoyancy. Journal of Geophysical Research B1, 313–323.

Wallace, P.J., Carmichael, I.S.E., 1994. S speciation in submarine basaltic glasses as determined by measurements of S$K\alpha$ X-ray wavelength shifts. American Mineralogist 79, 161–167.

Wallace, P.J., Anderson, A.T.J., Davis, A.M., 1999. Gradients in H_2O, CO_2, and exsolved gas in a large-volume silicic magma system: interpreting the record preserved in melt inclusions from the Bishop Tuff. Journal of Geophysical Research 104 (B9), 20097–20122.

Wilson, C.J.N., Hildreth, W., 1997. The Bishop Tuff: new insights from eruptive stratigraphy. Journal of Geology 105, 407–439.

Witter, J.B., 2003. Convection of magma in volcanic conduits as a

degassing mechanism at active volcanoes, Ph.D. Thesis, University of Washington.

Witter, J.B., Kress, V.C., Delmelle, P., Stix, J., 2004a. Volatile degassing, petrology and magma dynamics of the Villarrica Lava Lake, Southern Chile. Journal of Volcanology and Geothermal Research 134, 303–337.

Witter, J.B., Kress, V.C., Newhall, C.G., 2004b. Volcán Popocatépetl, Mexico: Petrology, magma missing and Immediate sources of volatiles for the 1994-present eruption. Journal of Petrology (in press).